Pseudospectral methods provide fast and accurate solutions for the horizontal infiltration equation

Simon A. Mathias[a,*], Graham C. Sander[b]

[a]*Department of Engineering, Durham University, Durham, UK*
[b]*School of Architecture, Building and Civil Engineering, Loughborough University, Loughborough, UK*

Abstract

An extremely fast and accurate pseudospectral numerical method is presented, which can be used in inverse methods for estimating soil hydraulic parameters from horizontal infiltration or desorption experiments. Chebyshev polynomial differentiation in conjunction with the flux concentration formulation of Philip (1973) results in a numerical solution of high order accuracy that is directly dependent on the number of Chebyshev nodes used. The level of accuracy ($< 0.01\%$ for 100 nodes) is confirmed through a comparison with two different, but numerically demanding, exact closed-form solutions where an infinite derivative occurs at either the wetting front or the soil surface. Application of our computationally efficient method to estimate soil hydraulic parameters is found to take less than one second using modest laptop computer resources. The pseudospectral method can also be applied to evaluate analytical approximations, and in particular, those of Parlange and Braddock (1980) and Parlange et al (1994) are chosen. It is shown that both these approximations produce excellent estimates of both the sorptivity and moisture profile across a wide range of initial and boundary conditions and numerous physically realistic diffusivity functions.

Keywords: Sorptivity, Infiltration, Analytical solution, Pseudospectral, Chebyshev

*Corresponding author. E-mail address: s.a.mathias@durham.ac.uk

1. Introduction

Since the 1970's, there have been numerous publications on approximate analytical solutions for determining both the sorptivity and moisture content profiles associated with horizontal infiltration. Many of these approximations (e.g. Parlange, 1971, 1975; Philip, 1973; Babu, 1976; Parlange and Braddock, 1980; Parslow et al., 1998; Parlange et al., 1994) require multiple integrals to be evaluated, iteration or multiple terms in a perturbation expansion to obtain the saturation profile. However, they do apply for arbitrary soil hydraulic properties. While other approximations (e.g. Ma et al., 2009; Tzimopoulos et al., 2015; Su et al., 2017; Sadeghi et al., 2017; Su et al., 2018; Hayek, 2018) provide simple closed-form approximations, these are for either a very specific soil moisture characteristic equation (Brooks and Corey, 1964; Gardner, 1958), hydraulic diffusivity (exponential) or flux concentration relation (Philip, 1973).

In the case of the widely used van Genuchten (1980) model of the soil moisture characteristic equation, a simple closed form solution for the moisture content profile was found by Zimmerman and Bodvarsson (1989) by using boundary layer theory at the wetting front. Interestingly their solution was capable of handling both ponded and unsaturated surface boundary conditions for an arbitrary constant initial condition. However the accuracy of their method reduced significantly for near dry initial conditions. The size of this error was subsequently decreased by Parlange et al. (1991) through combining his earlier optimization results (Parlange, 1975) with an approximation for the profile developed by Brutsaert (1976).

The level of accuracy of the approximate analytical solutions arises from the nature of the limiting assumptions that are made about the moisture content profile. Their advantage though, as compared to numerically evaluating an exact solution to the full problem, is predominantly a saving in computation time that significantly increases as greater accuracy is sought. This is where pseudospectral methods come into their own as an accurate and computationally efficient method for obtaining a numerical solution to the dual problem of determining sorptivity and moisture content profiles. One of the main benefits of a pseudospectral method is that the error diminishes rapidly as the number of nodal points increase (Fornberg, 1998), such that the resulting solution can be readily integrated or differentiated, to the same order of accuracy as the original solution. Such a method was successfully developed by Bjørnarå and Mathias (2013) to solve a related and similar problem of two-phase flow due to McWhorter and Sunada (1990).

We have four objectives for this article. The first is to demonstrate the benefits of using a pseudospectral method to study the horizontal infiltration equation. The second is to use a pseudospectral method to, not only develop an essentially exact numerical solution to the full problem utilizing the flux concentration formulation of Philip and Knight (1974), but also to show how it can be used to evaluate existing approximate analytical solutions. In particular, we choose the approximate solutions developed by Parlange and Braddock (1980) and Parlange et al. (1994) because: (1) they are straightforward to apply in a pseudospectral formulation and (2) they provide a level of accuracy for both the sorptivity and the moisture profile for an arbitrary diffusivity that has not been subsequently surpassed.

Inverse methods are well known for being computationally demanding and faster more accurate and efficient methods are always being sought after. Thus our third objective is to demonstrate how the computational speed and accuracy of our pseudospectral method can be exploited for the rapid inverse determination of estimating soil hydraulic parameters from horizontal infiltration experiments.

Typically, it is more common for vertical infiltration rather than horizontal infiltration experiments to be used for inverse modelling of hydraulic parameters. However, during drying or desorption experiments, hydraulic gradients will dominate the flow of water and neglecting the effects of gravity can be justified. Consequently, our final objective is to demonstrate that our methodology is straightforward to apply and maintains high levels of accuracy for desorption scenarios as well.

The outline of this article is as follows. First we present the governing equations for the horizontal infiltration boundary value problem. The Boltzmann transform is applied to obtain the flux concentration formulation of Philip and Knight (1974). It is explained how to evaluate two approximate analytical solutions and a flux concentration solution using a Chebyshev polynomial differentiation matrix. In particular we choose the approximations of Parlange and Braddock (1980) and Parlange et al. (1994) as they apply for arbitrary diffusivity functions and have previously been shown to be quite accurate. An error analysis is performed by comparison to exact closed-form solutions for two special diffusivity functions from Philip (1960). Computation times for both the approximate solutions and the flux concentration solution are studied as a function of number of Chebyshev nodes. The solutions are again compared when using the van Genuchten (1980) soil moisture characteristic equations. We then present an example whereby the pseudospectral flux concentration solution is used for the rapid and accurate inverse modelling of a horizontal infiltration experiment dataset from Villarreal et al. (2019). Finally we compare some desorption results from our pseudospectral flux concentration solution with numerical results previously obtained by Lisle et al. (1987).

2. Methods and data

2.1. Governing equations

Horizontal infiltration is described by the mass conservation equation

$$\frac{\partial \theta}{\partial t} = -\frac{\partial q}{\partial x} \tag{1}$$

with the moisture flux, q [LT^{-1}], being found from Darcy's law

$$q = -D(\theta)\frac{\partial \theta}{\partial x} \tag{2}$$

where θ [-] is moisture content, t [T] is time, x [L] is distance and $D(\theta)$ [L^{2}T^{-1}] is the hydraulic diffusivity.

We consider solutions of Eqs. (1) and (2) subjected to the following initial and boundary conditions:

$$\begin{aligned} &\theta = \theta_I, \quad x \geq 0, \quad && t = 0 \\ &\theta = \theta_0, \quad x = 0, \quad && t > 0 \\ &\theta = \theta_I, \quad x \to \infty, \quad && t > 0 \end{aligned} \tag{3}$$

where θ_I [-] is a uniform initial moisture content value and θ_0 [-] is a constant boundary moisture content value.

The cumulative infiltration of fluid, V [L], through $x = 0$ is found from (Philip, 1957)

$$V = -\int_0^t D(\theta_0) \left.\frac{\partial \theta}{\partial x}\right|_{x=0} dt = S t^{1/2} \tag{4}$$

where S [LT$^{-1/2}$] is the sorptivity.

2.1.1. Application of dimensionless transforms and Boltzmann transform

To aid further study we introduce the following dimensionless transformations:

$$\vartheta = \frac{\theta - \theta_r}{\theta_s - \theta_r}, \quad \overline{D} = \frac{(\theta_s - \theta_r)D}{K_s \psi_c}, \quad \sigma = \frac{S}{\sqrt{(\theta_s - \theta_r)K_s\psi_c}} \tag{5}$$

along with a dimensionless Boltzmann transform

$$\phi = \sqrt{\frac{(\theta_s - \theta_r)x^2}{K_s \psi_c t}} \tag{6}$$

where θ_r [-] and θ_s [-] are the residual and saturated moisture contents, K_s [LT^{-1}] is the saturated hydraulic conductivity and ψ_c [L] represents the capillary length scale of the porous medium of concern.

The boundary value problem above then reduces to

$$-\frac{\phi}{2}\frac{d\vartheta}{d\phi} = \frac{d}{d\phi}\left(\overline{D}(\vartheta)\frac{d\vartheta}{d\phi}\right) \tag{7}$$

subjected to the following boundary conditions:

$$\begin{aligned} \vartheta &= \vartheta_I, \quad \phi \to \infty \\ \vartheta &= \vartheta_0, \quad \phi = 0 \end{aligned} \tag{8}$$

whilst the dimensionless sorptivity can be found from (Philip, 1969)

$$\sigma = \int_{\vartheta_I}^{\vartheta_0} \phi(\vartheta) d\vartheta \tag{9}$$

For the commonly applied form of soil moisture characteristic equations attributed to van Genuchten (1980), the dimensionless diffusivity is given by

$$\overline{D}(\vartheta) = \left(\frac{1-m}{m}\right) \vartheta^{L-1/m} \frac{\left[1 - \left(1 - \vartheta^{1/m}\right)^m\right]^2}{(1 - \vartheta^{1/m})^m} \tag{10}$$

where L and m are empirical parameters. The L parameter is normally taken to be 0.5 (as is assumed hereafter in this article) and $m \in (0, 1)$.

2.1.2. Flux concentration formulation

For cases where $\overline{D}(\vartheta = \vartheta_I) = 0$, ϕ has compact support, meaning $\phi \in [0, \phi_f]$ where ϕ_f denotes the location of a discrete wetting front. However, when using the van Genuchten (1980) diffusivity function with $\theta_I > 0$, it will be the case that $\overline{D}(\vartheta = \vartheta_I) > 0$ and $\phi \in [0, \infty)$.

A problem with directly solving Eq. (7) using a Chebyshev differentiation matrix is that, in the case where there is a semi-infinite independent variable, $\phi \in [0, \infty)$, it must be mapped to the finite region of the Chebyshev space, $z \in [-1, 1]$. One way to avoid this is to multiply both sides of Eq. (7) by $d\phi/d\vartheta$ such that $\phi \in [0, \infty)$ and $\vartheta \in [\vartheta_I, \vartheta_0]$ become the new dependent and independent variables, respectively (Philip, 1955). The ϑ variable can be easily mapped to the z-space via a linear transform. In this article we obtain a pseudospectral solution using the flux concentration formulation of Philip (1973), which utilizes independent and dependent variables that are both bounded by finite limits.

The flux concentration, F [-], is defined by (Philip and Knight, 1974)

$$F \equiv \frac{q(x,t)}{q(0,t)} = -\frac{2\overline{D}(\vartheta)}{\sigma}\frac{d\vartheta}{d\phi} \tag{11}$$

which, on substitution into Eq. (7), leads to the boundary value problem (Philip and Knight, 1974):

$$\frac{d^2F}{d\vartheta^2} = -\frac{2\overline{D}(\vartheta)}{\sigma^2 F} \tag{12}$$

$$\begin{aligned} F &= 1, \quad \vartheta = \vartheta_0 \\ F &= 0, \quad \vartheta = \vartheta_I \end{aligned} \tag{13}$$

Given a solution for F, the dimensionless sorptivity, σ, is found from (Philip and Knight, 1974)

$$\sigma^2 = 2\int_{\vartheta_I}^{\vartheta_0} \frac{(\vartheta - \vartheta_I)\overline{D}(\vartheta)}{F} d\vartheta \tag{14}$$

and ϕ can be found from (Philip, 1973)

$$\phi = \sigma \frac{dF}{d\vartheta} \tag{15}$$

An apparent problem is that a value of σ is needed to obtain a solution for F. However, this is easily dealt with by evaluating F and σ, simultaneously, within a single Newton iteration scheme. Bjørnarå and Mathias (2013) employed a very similar scheme to solve a two-phase flow problem previously defined by McWhorter and Sunada (1990).

2.2. *Chebyshev spectral collocation (pseudospectral) method*

In this article, values of ϕ, for both a flux concentration solution and the approximate solutions of Parlange and Braddock (1980) and Parlange et al. (1994), are obtained using a pseudospectral differentiation matrix, $\mathbf{D}$, which is a matrix such that the values of the d'th derivative of a function $y(\mathbf{z})$ at distinct nodes $\mathbf{z}$ can be approximated by $y^{(d)}(\mathbf{z}) \approx \mathbf{D}^{(d)} y(\mathbf{z})$. Following Bjørnarå and Mathias (2013) we adopt a Chebyshev polynomial differentiation matrix (Weideman and Reddy, 2000).

The Chebyshev polynomial of the second kind, p, interpolates a function, y, at the nodes (so-called Chebyshev nodes) (Weideman and Reddy, 2000, p. 479)

$$z_k = \cos\left(\frac{(k-1)\pi}{N-1}\right), \quad k = 1, 2, \ldots, N \tag{16}$$

such that $p(\mathbf{z}) = y(\mathbf{z})$. Note that $z \in [-1, 1]$.

The value of the interpolating polynomial's d'th derivative at the k'th node is given by (Weideman and Reddy, 2000):

$$p^{(d)}(\mathbf{z}) = \mathbf{D}^{(d)} y(\mathbf{z}) \tag{17}$$

where $\mathbf{D}^{(d)}$ is the d'th order Chebyshev differentiation matrix. We use a short MATLAB code called CHEBDIF, provided by Weideman and Reddy (2000), for creating the Chebyshev points, $\mathbf{z}$, and the differentiation matrix, $\mathbf{D}$.

2.2.1. *Imposing Dirichlet boundary conditions*

In the differentiation matrix method for solving differential equations, the interpolating polynomial is only required to satisfy the differential equation at the interior nodes. The values of the interpolating polynomial and the derivatives at the interior nodes are, respectively (Piché, 2007; Piché and Kanniainen, 2009):

$$p(\mathbf{z}_{2:N-1}) = y(\mathbf{z}_{2:N-1}) = \mathbf{I}_{2:N-1,:}\mathbf{y} \tag{18}$$

$$p^{(d)}(\mathbf{z}_{2:N-1}) = \mathbf{D}^{(d)}_{2:N-1,:}\mathbf{y} \tag{19}$$

where $\mathbf{I}$ is the identity matrix.

Piché (2007) and Piché and Kanniainen (2009) use a sub-matrix notation associated with MATLAB. The $\mathbf{z}_{2:N-1}$ term represents all rows of the vector, $\mathbf{z}$, except for the first and last rows. The $\mathbf{I}_{2:N-1,:}$ term represents all rows of an identity matrix except for the first and last rows. The $\mathbf{D}^{(d)}_{2:N-1,:}$ term represents all rows of a dth order differentiation matrix except for the first and last rows.

Dirichlet boundary conditions can be specified as constraints on the end nodes, corresponding to the first and last rows of the differentiation matrix, i.e.:

$$\begin{aligned} p(z = 1) &= y_1 \\ p(z = -1) &= y_N \end{aligned} \tag{20}$$

2.2.2. *Mapping the Chebyshev nodes to the solution space*

The coordinate space for the Chebyshev nodes is $z \in [-1, 1]$ (note that $z_N = -1$ and $z_1 = 1$). However, the solution space for the normalised moisture content is $\vartheta \in [\vartheta_I, \vartheta_0]$. Therefore, the Chebyshev nodes, z_k, need to be mapped to the normalised moisture content space by the following transform:

$$\vartheta = \frac{\vartheta_0 + \vartheta_I}{2} + \frac{\vartheta_0 - \vartheta_I}{2} z \tag{21}$$

Here we also introduce an appropriately transformed differentiation matrix, $\mathbf{E}$, where

$$\mathbf{E} = \frac{dz}{d\vartheta}\mathbf{D} \tag{22}$$

and, from Eq. (21)

$$\frac{dz}{d\vartheta} = \frac{2}{\vartheta_0 - \vartheta_I} \tag{23}$$

2.2.3. *Evaluating definite integrals*

Once a variable, $f(y \in [a, b])$, is specified at the Chebyshev nodes, it can be integrated using a Lobatto-type integration formula (previously explained by Bjørnarå and Mathias, 2013):

$$\int_a^b f(y)dy \approx \frac{\pi}{N-1}\left(\frac{b-a}{2}\right)\sum_{k=1}^{N} \sqrt{1 - z_k^2} f_k \tag{24}$$

where z_k are the locations of the Chebyshev nodes given in Eq. (16) and $f_k = f(z_k)$.

2.3. Pseudospectral solution of the horizontal infiltration equation

Here we explain how to evaluate a pseudospectral solution of the horizontal infiltration equation using the flux concentration formulation of Philip (1973).

By applying Eq. (19) on the interior nodes and Dirichlet boundary conditions and Eq. (20), on the end-nodes, Eq. (12) can be written in matrix form (similar to Piché, 2007):

$$\mathbf{R}(\mathbf{F}) = \begin{bmatrix} \mathbf{E}^{(2)}_{2:N-1,:}\mathbf{F} + \mathbf{I}_{2:N-1,:}\left[\dfrac{2\overline{D}}{\sigma^2 F}\right] \\ F_N - 0 \\ F_1 - 1 \end{bmatrix} \tag{25}$$

where $\mathbf{R}$ is the residual vector, $\mathbf{F}$ represents the solution vector for the dependent variable, F, $\left[\frac{2\overline{D}}{\sigma^2 F}\right]$ is a vector containing a value for every Chebyshev node, and the two last rows impose the Dirichlet boundary conditions, Eq. (13), on F.

2.3.1. Newton's iteration method

Eq. (25) must be solved iteratively. Let $\mathbf{F}_i$ be the i-th iteration of the solution vector. The residual vector for the subsequent iteration, $\mathbf{R}(\mathbf{F}_{i+1})$, satisfies the Taylor series:

$$\mathbf{R}(\mathbf{F}_{i+1}) = \mathbf{R}(\mathbf{F}_i) + \left[\frac{\partial \mathbf{R}}{\partial \mathbf{F}_i}\right]\Delta\mathbf{F} + O(\Delta\mathbf{F}^2) \tag{26}$$

where $\Delta\mathbf{F} = \mathbf{F}_{i+1} - \mathbf{F}_i$ and $[\partial\mathbf{R}/\partial\mathbf{F}_i]$ is the Jacobian matrix found from (similar to Piché, 2007)

$$\left[\frac{\partial\mathbf{R}}{\partial\mathbf{F}_i}\right] = \begin{bmatrix} \mathbf{E}^{(2)}_{2:N-1,:} + \mathbf{I}_{2:N-1,:}\mathrm{diag}\left(\left[-\dfrac{2\overline{D}}{\sigma^2 F^2}\right]\right) \\ \mathbf{I}_{N,:} \\ \mathbf{I}_{1,:} \end{bmatrix} \tag{27}$$

where $\left[-\frac{2\overline{D}}{\sigma^2 F^2}\right]$ is a vector containing a value for every Chebyshev node.

If $\mathbf{F}_{i+1}$ is the exact solution then $\mathbf{R}(\mathbf{F}_{i+1}) = 0$ and we should obtain $\Delta\mathbf{F}$ from

$$\Delta\mathbf{F} = -\left[\frac{\partial\mathbf{R}}{\partial\mathbf{F}_i}\right]^{-1}\mathbf{R}(\mathbf{F}_i) + O(\Delta\mathbf{F}^2) \tag{28}$$

To reach this goal, we therefore update $\mathbf{F}$ using the Newton iteration

$$\mathbf{F}_{i+1} = \mathbf{F}_i - \left[\frac{\partial\mathbf{R}}{\partial\mathbf{F}_i}\right]^{-1}\mathbf{R}(\mathbf{F}_i) \tag{29}$$

The scheme can be considered to have converged when $|\Delta\mathbf{F}|$ has reached an acceptably low level.

Note that at the interior nodes, $F \in (0, 1)$. Therefore a good initial guess is to set $\mathbf{F} = 1$. An additional "correction"-step in the Newton iteration loop must also be applied to ensure the positivity condition, $F > 0$. The iteration loop is continued until $\max(|\Delta\mathbf{F}|) < 10^{-6}$.

2.3.2. Evaluation of the sorptivity

The dimensionless sorptivity is determined by evaluating the integral in Eq. (14) using Eq. (24), i.e.:

$$\sigma^2 = \frac{\pi}{N-1}\left(\frac{\vartheta_0 - \vartheta_I}{2}\right)\sum_{k=1}^{N}\sqrt{1-z_k^2}\left[\frac{2(\vartheta - \vartheta_I)\overline{D}}{F}\right]_k \tag{30}$$

The dimensionless sorptivity, σ, is iteratively found for a given ϑ_0 such that $F(\vartheta_0) = 1$. Therefore, σ needs to be evaluated in each Newton iteration so that the two variables F and σ converge to a solution.

An example MATLAB script for the above procedures is provided as an appendix below.

2.4. Closed-form exact solutions

Two closed-form exact solutions, due to Philip (1960), utilizing specialised diffusivity functions, will be used to assess the error associated with our pseudospectral solution described above.

Case 1 has compact support (or a finite wetting front) with an infinite spatial derivative at the front. This type of infiltrating front is very demanding for any numerical discretization method and provides a stringent test on its accuracy. In contrast, Case 2 has an infinite derivative at the surface boundary. These two exact solutions therefore allow the assessment of our numerical method under two very different but extremely demanding flow conditions.

2.4.1. Case 1

For the special case when $\vartheta_I = 0$, $\vartheta_0 = 1$ and

$$\overline{D} = \frac{m\vartheta^m}{2}\left(1 - \frac{\vartheta^m}{m+1}\right), \quad m > 0 \tag{31}$$

where m [-] is an empirical exponent, it can be shown that (Philip, 1960)

$$\phi = 1 - \vartheta^m \tag{32}$$

and consequently, from Eqs. (9) and (15), respectively:

$$\sigma = \frac{m}{m+1} \tag{33}$$

$$F = \frac{(m+1)\vartheta - \vartheta^{m+1}}{m} \tag{34}$$

2.4.2. Case 2

For the special case when $\vartheta_I = 0$, $\vartheta_0 = 1$ and

$$\overline{D} = \frac{m}{2(m+1)}\left[(1-\vartheta)^{m-1} - (1-\vartheta)^{2m}\right], \quad m > 0 \tag{35}$$

where m [-] is an empirical exponent, it can be shown that (Philip, 1960)

$$\phi = (1 - \vartheta)^m \tag{36}$$

and consequently, from Eqs. (9) and (15), respectively:

$$\sigma = \frac{1}{m+1} \tag{37}$$

$$F = 1 - (1-\vartheta)^{m+1} \tag{38}$$

2.5. Parlange's approximation

A number of different approximate solutions for general diffusivity functions have been developed. Arguably the most accurate of these are due to Parlange and Braddock (1980) and Parlange et al. (1994). The advantage of employing an approximate solution over a solution to the full problem is that the computation time is reduced. In this article we compare the computation time for our pseudospectral flux concentration solution with that required to evaluate the approximate solutions of Parlange and Braddock (1980) and Parlange et al. (1994).

2.5.1. Parlange and Braddock (1980) approximation

The approximation of Parlange and Braddock (1980) gives that ϕ is found from:

$$\phi = AU \tag{39}$$

where

$$A^2 = \frac{2\int_{\vartheta_I}^{\vartheta_0} \overline{D} d\vartheta}{\int_{\vartheta_I}^{\vartheta_0} U^2 d\vartheta} \tag{40}$$

$$\frac{dU}{d\vartheta} = B \tag{41}$$

and

$$B = \frac{\overline{D}}{\vartheta - \vartheta_I}\left[\frac{1}{n+1}\left(\frac{\vartheta - \vartheta_I}{\vartheta_0 - \vartheta_I} - 1\right)^n\right]^{-1} \tag{42}$$

where n satisfies

$$\frac{\int_{\vartheta_I}^{\vartheta_0}(\vartheta - \vartheta_I)\overline{D}d\vartheta}{\int_{\vartheta_I}^{\vartheta_0}(\vartheta_0 - \vartheta_I)\overline{D}d\vartheta} = \frac{1}{4}\frac{(2n+3)(2n+1)}{(n+1)(n+2)} \tag{43}$$

A value for sorptivity can be obtained by substituting Eq. (39) into Eq. (9).

2.5.2. *Parlange et al. (1994) approximation*

The approximation of Parlange et al. (1994) gives that ϕ satisfies the equation:

$$\frac{A}{2}\phi^2 + \frac{\sigma}{\vartheta_0 - \vartheta_I}\phi + 2U = 0 \tag{44}$$

where

$$\frac{dU}{d\vartheta} = B \tag{45}$$

$$B = \frac{\overline{D}}{\vartheta - \vartheta_I} \tag{46}$$

and

$$\sigma^2 = (2 - A)(\vartheta_0 - \vartheta_I)\int_{\vartheta_I}^{\vartheta_0} \overline{D} d\vartheta \tag{47}$$

where A is a constant satisfying the equation

$$\frac{(2 - A)(2 + nA)}{2(1 + nA)[2 + (n - 1)A]} = \frac{\int_{\vartheta_I}^{\vartheta_0} (\vartheta - \vartheta_I)^n \overline{D} d\vartheta}{\int_{\vartheta_I}^{\vartheta_0} (\vartheta_0 - \vartheta_I)^n \overline{D} d\vartheta} \tag{48}$$

and

$$n + 0.72068 = \frac{\int_{\vartheta_I}^{\vartheta_0} (\vartheta_0 - \vartheta_I) \overline{D} d\vartheta}{\int_{\vartheta_I}^{\vartheta_0} (\vartheta_0 - \vartheta) \overline{D} d\vartheta} \tag{49}$$

2.5.3. *Evaluation by pseudospectral method*

The approximate solutions of Parlange and Braddock (1980) and Parlange et al. (1994) also lend themselves to evaluation by pseudospectral method. The definite integrals can be evaluated using Eq. (24). The U term can be evaluated using the Chebyshev differentiation matrix, with the constraint that $U = 0$ at $\vartheta = \vartheta_0$, by solving the following system of equations:

$$\mathbf{U} = \begin{bmatrix} \mathbf{E}^{(1)}_{2:N,:} \\ \\ \mathbf{I}_{1,:} \end{bmatrix}^{-1} \begin{bmatrix} \mathbf{B}_{2:N} \\ \\ 0 \end{bmatrix} \tag{50}$$

where $\mathbf{U}$ and $\mathbf{B}$ are vectors of U and B values that correspond to each Chebyshev node, respectively. The B values are found from Eq. (42) for the Parlange and Braddock (1980) approximation and from Eq. (46) for the Parlange et al. (1994) approximation.

2.6. Experimental data and its analysis

To demonstrate the applicability of our pseudospectral flux concentration solution for inverse modelling, we revisit the horizontal infiltration data previously presented by Villarreal et al. (2019). Villarreal et al. (2019) studied three different soils from the Argentinean Pampas Region: a silty loam, a loam and a sandy loam. Disturbed soil samples were air dried to a mean initial moisture content of between 0.03 and 0.07, sieved through a 2-mm mesh and then gently packed into PVC tubes of 35 cm length and 10 cm interior diameter. The tubes were horizontally orientated with a water inlet boundary at one end, where the water pressure was held at atmospheric pressure, and an impermeable boundary at the other end. The cumulative infiltration along with the soil moisture content at 15, 20 and 25 cm from the inlet boundary were monitored continuously with time.

Model parameter values for our pseudospectral solution can be obtained by calibration against this observed experimental data as follows. First, the sorptivity, S [$\mathrm{LT}^{-1/2}$], is obtained by linear regression of the infiltration time-series data. Values for the van Genuchten (1980) m parameter and the quantities θ_r and $(\theta_s - \theta_r)$ are guessed. The normalised initial and boundary moisture contents, ϑ_I and ϑ_0 are assumed to be 0.001 and 0.999, respectively, to reflect the air-dried initial condition and atmospheric boundary, respectively. A value for σ along with corresponding ϕ values, denoted $\boldsymbol{\phi}$, at the locations in Chebyshev space, $\mathbf{z}$, of 100 Chebyshev nodes, are determined using the pseudospectral flux concentration solution described above.

The locations of the observed moisture contents, θ_j, in Chebyshev space, z_j, are determined from (recall Eq. (21))

$$z_j = \frac{2(\theta_j - \theta_r) - (\theta_s - \theta_r)(\vartheta_0 + \vartheta_I)}{(\theta_s - \theta_r)(\vartheta_0 - \vartheta_I)} \tag{51}$$

Corresponding values of ϕ, denoted ϕ_j, are obtained by interpolating $\boldsymbol{\phi}$ using a MATLAB function, called CHEBINT (available from Weideman and Reddy, 2000), which uses Chebyshev polynomials to provide an exact interpolation of the pseudospectral solution (Weideman and Reddy, 2000).

The corresponding "modelled" times of each experimental value, t_j, can then be determined from

$$t_j = \frac{(\theta_s - \theta_r)x_j^2}{K_s\psi_c\phi_j^2} \tag{52}$$

where x_j is the distance from the boundary inlet at which the moisture content was recorded and a value for the product $K_s\psi_c$ $[\mathrm{L}^2\mathrm{T}^{-1}]$ is obtained from

$$K_s\psi_c = \frac{S^2}{(\theta_s - \theta_r)\sigma^2} \tag{53}$$

New values of m, θ_r and $(\theta_s - \theta_r)$ are iteratively selected by MATLAB's optimisation routine, FMINSEARCH, and the process above is repeated, until the mean absolute error (MAE), between values of $t_j^{1/2} x_j^{-1}$ from the experimental observation record and those determined from Eq. (52), is minimised.

FMINSEACH uses the Nelder-Mead simplex algorithm as described by Lagarias et al. (1998). Seed values for the unknown parameters are determined as follows. The seed value for m is arbitrarily taken to be 0.2 and for θ_r it is taken to be the minimum observed soil moisture content in the data. The seed value for $(\theta_s - \theta_r)$ is taken to be the difference between the maximum and minimum observed soil moisture content in the data.

3. Results

Here we present results using pseudospectral implementations of the Parlange approximations and the pseudospectral flux concentration solution for the horizontal infiltration equation. First we assess the error of the different approaches by comparison with the two closed-form exact solutions of Philip (1960). We then compare the computation time required for the different schemes, using the van Genuchten (1980) diffusivity function. We provide a demonstration, where the pseudospectral flux concentration solution is used to inverse model hydraulic parameters from the experimental horizontal infiltration data from Villarreal et al. (2019). Finally, it is shown how our methodology can also be easily applied to desorption scenarios and our results are compared with those from Lisle et al. (1987).

3.1. Comparison with the closed-form exact solutions of Philip (1960)

A comparison with the closed-form exact solutions of Philip (1960) was performed to verify the accuracy of the pseudospectral flux concentration solution. Fig. 1 shows results for Case 1, where $\phi = 1-\vartheta^m$. Figs.1a and b show plots of flux concentration, F, and dimensionless Boltzmann transform, ϕ, respectively, for various values of m. Whereas the ϑ distribution with ϕ is important for simulating horizontal infiltration experiments, the F plots are interesting because this is the dependent variable being solved for within the Newton iteration scheme (recall Eq. (12)).

For Figs.1a and b, the pseudospectral flux concentration solution was evaluated using 30 Chebyshev nodes. The Philip (1960) solution was evaluated at the same Chebyshev nodes and the results are shown as circular markers. The location of the circular markers in Figs. 1a and b therefore also show the location of these Chebyshev nodes. The cosine distribution of the nodes leads to a natural clustering of nodes at both the boundary condition and the wetting front. It can be seen that there is close to perfect correspondence between both solutions for all the m values studied. Values of ϕ were also determined using the approximate solutions of Parlange and Braddock (1980) and Parlange et al. (1994), using the same 30 Chebyshev nodes, and these are found to be indistinguishable from the flux concentration solution. However we also note that the approximate solution of Parlange and Braddock (1980), yields the exact analytical solution of Eq. (32) when the diffusivity is given by Eq. (31).

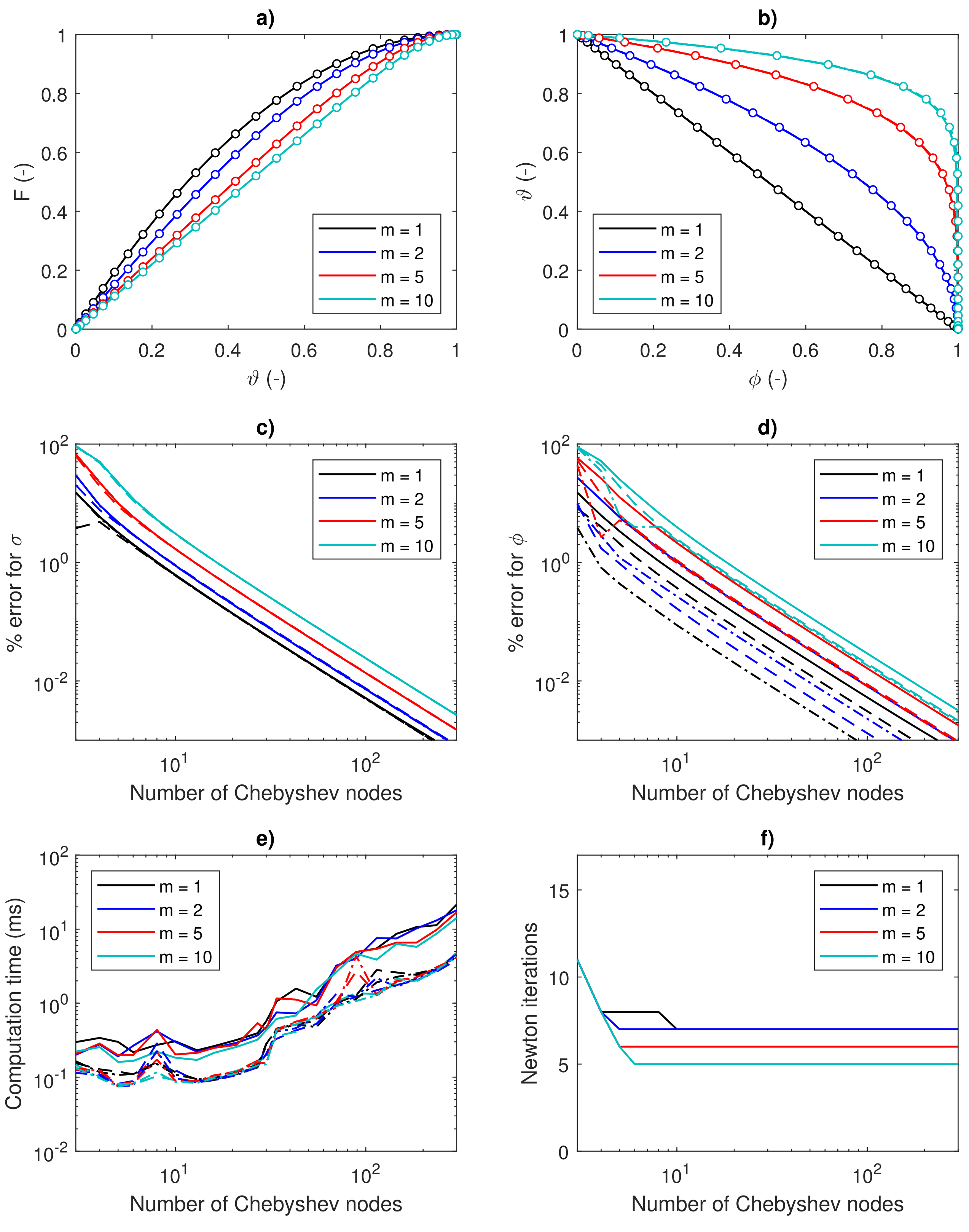

Figure 1: a) Plots of flux concentration against normalised moisture content ϑ (only for the flux concentration solution and exact closed form solution) for different m values, using the Case 1 diffusivity function of Philip (1960). b) Plots of normalised moisture content against dimensionless Boltzmann transform. c) Plots of % error for dimensionless sorptivity, σ. d) Plots of mean % error for dimensionless Boltzmann transform, ϕ. e) Plots of computation time against number of Chebyshev nodes. f) Plots of number of Newton iterations against Chebyshev nodes (only for the flux concentration solution). Circular markers are from the exact closed-form solution of Philip (1960) for Case 1. The solid, dashed and dashed-dot lines are from the flux concentration solution, the Parlange and Braddock (1980) approximation and the Parlange et al. (1994) approximation, respectively.

A sensitivity analysis was performed to explore how the number of Chebyshev nodes, N, affects the accuracy of the solutions. Figs. 1c and d show plots of percentage error in terms of dimensionless sorptivity, σ, and dimensionless Boltzmann transform, ϕ. These errors were calculated from the difference between the pseudospectral solutions/approximations and the closed-form exact solution of Philip (1960). For ϕ, the percentage error was taken to be the mean absolute error for each Chebyshev node divided by the mean value of ϕ for each Chebyshev node, according to the closed-form exact solution. The errors can be seen to progressively reduce, with increasing N, for both the pseudospectral flux concentration solution and Parlange's approximations.

All simulations reported in this article were conducted on a Lenovo Thinkpad with an Intel Core i5-835OU CPU at 1.70 GHz. Fig. 1e shows plots of computation time as a function of N. The pseudospectral flux concentration solution typically requires between three and six times the amount of time as compared to Parlange's approximations. The main reason for this is that the flux concentration solution involves a Newton iteration scheme requiring between 5 and 11 iterations (see Fig. 1f). Nevertheless, this still takes less than 30 ms to compute, even with 300 Chebyshev nodes.

With the Parlange and Braddock (1980) method being exact for this example, the errors shown in Figs. 1c and d are purely due to the truncation errors associated with the evaluation of the integrals in Eqs. (40) and (43) using Eq. (24).

Fig. 2 shows results from repeating the above analysis but using Case 2 of Philip (1960), where $\phi = (1 - \vartheta)^m$. Again, the flux concentration solution provides a high level of accuracy and continuously improves with increasing number of Chebyshev nodes, N. In contrast, the error for the two approximate solutions reaches an irreducible value beyond which it no longer reduces with increasing N. This irreducible error is due to the limiting assumptions embedded in the derivations of these approximations. As both of the Parlange approximations are based on a sharp wetting front, then it is not surprising that their accuracy is much more limited for this diffusivity and the corresponding moisture profile. Actually, the surprising result here is that they therefore do as well as they do. The computation time for the flux concentration solution is between two and ten times that needed for the approximations. However, a solution with 30 nodes provides % errors in both σ and ϕ of less than 0.1% whilst taking less than 0.6 ms to compute.

The oscillations seen in the results from the Parlange et al. (1994) approximation, in Fig. 2b, are due to Gibbs phenomenon, resulting from the pseudospectral implementation. These oscillations were found to dampen to negligible levels when $N > 100$.

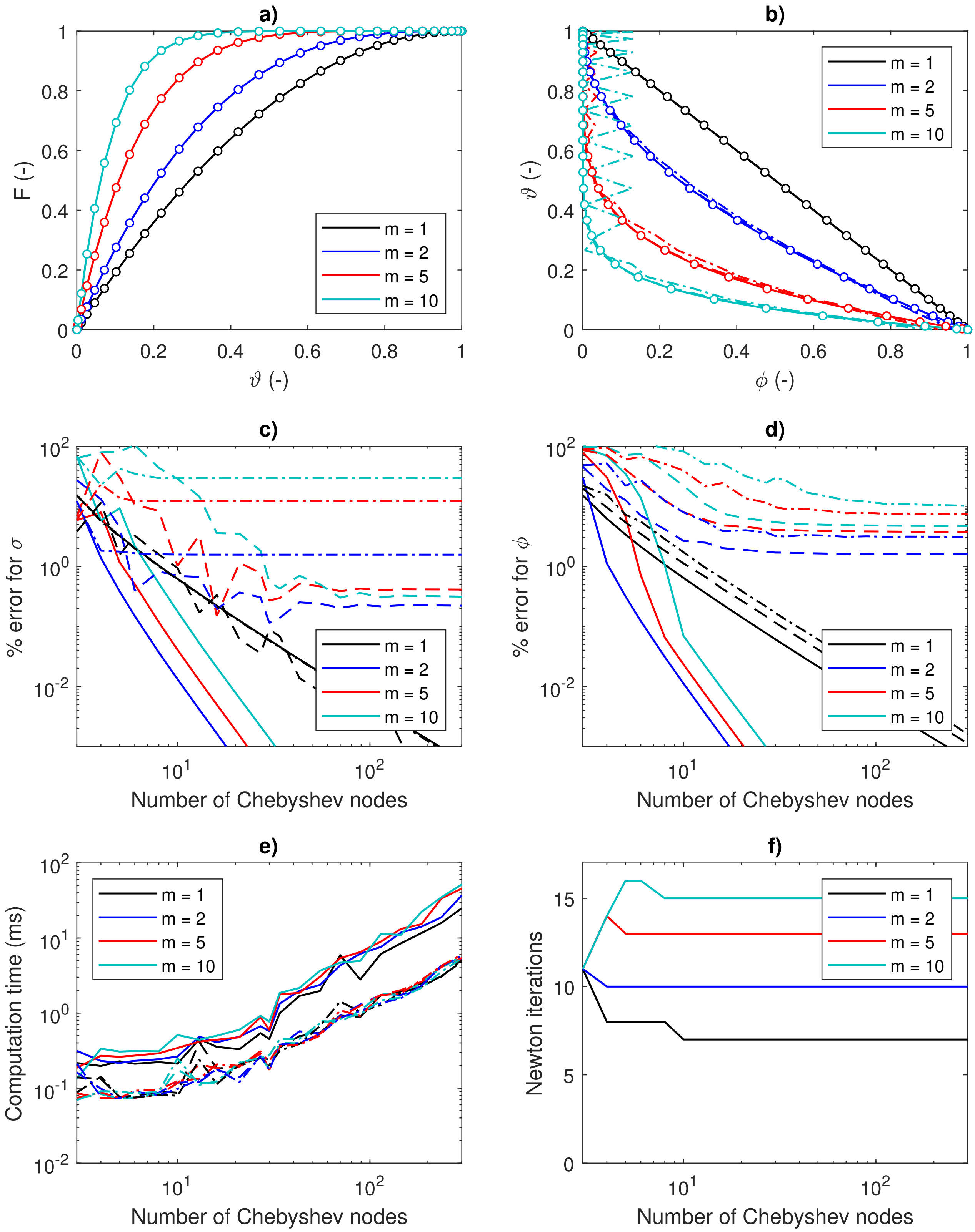

Figure 2: Same as Fig. 1 but for Case 2 of Philip (1960).

3.2. *Comparison of results using the van Genuchten diffusivity function*

Fig. 3 shows plots of normalised moisture content, ϑ, against normalised similarity transform, ϕ, for different values of ϑ_I, ϑ_0 and m, using the van Genuchten (1980) diffusivity function, given in Eq. (10), and 100 Chebyshev nodes. The pseudospectral flux concentration solution is shown as solid lines while the approximations of Parlange and Braddock (1980) and Parlange et al. (1994) are shown as dashed and dashed-dot lines, respectively. The approximations of Parlange and Braddock (1980) and Parlange et al. (1994) provide very close correspondence with the flux concentration solution, including where there is significant diffusion tailing. Indeed, it is not possible to visually distinguish between the Parlange and Braddock (1980) approximation and the flux concentration solution.

Additional numerical details relating to these simulations are presented in Table 1. Note that the sorptivity values are those calculated using the flux concentration solution. For all the scenarios studied, both of Parlange's approximations were able to provide sorptivity estimates with less than 0.3% error. It was found that the flux concentration solution required around four times as much computation time as compared to the approximations, but this was of the order of a few milliseconds.

While it is clear that both of Parlange's approximations are very accurate, the approximation of Parlange and Braddock (1980) is usually superior with estimating both σ and the moisture content profiles (Figs. 2b, c and Table 1) for the diffusivities presented here. Both methods use moments to determine an unknown parameter and then σ. However, the approximation of Parlange et al. (1994) is developed from a truncated expansion around the front whereas the approximation of Parlange and Braddock (1980) is not. We have carried out additional comparisons between the two Parlange approximations for both power law (ϑ^p) and exponential law ($e^{p\vartheta}$) diffusivities for $p = 0, 1, 2, 3 \ldots 10$. In both cases it was again found that the Parlange and Braddock (1980) approximation provided better estimates for the majority of p values. Nevertheless, the differences

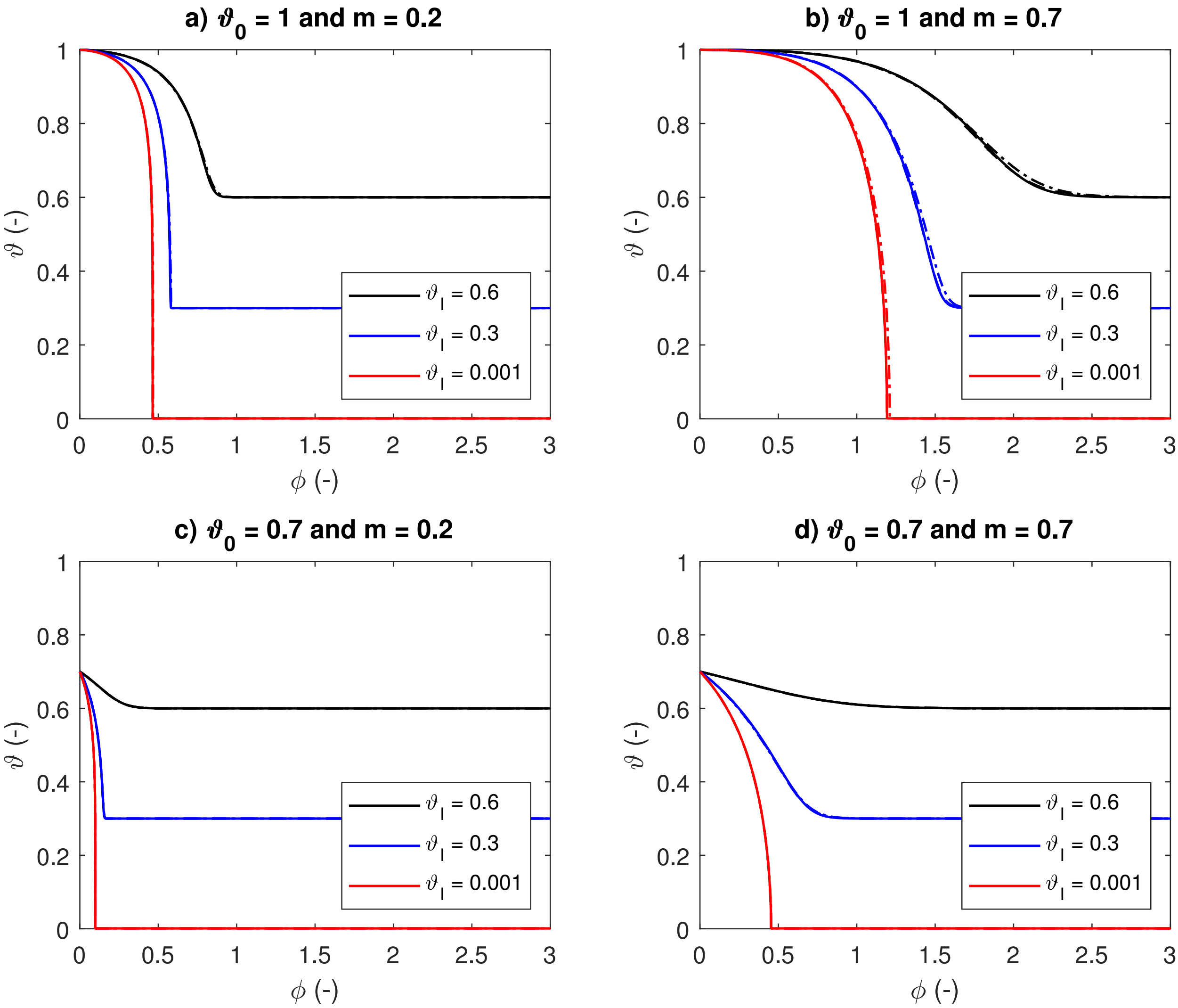

Figure 3: Plots of normalised moisture content, ϑ, against dimensionless similarity transform, ϕ, using the van Genuchten (1980) diffusivity function defined in Eq. (10), with ϑ_0 and m as specified in the subtitles and ϑ_I as specified in the legends. The solid, dashed and dashed-dot lines are from the flux concentration solution, the Parlange and Braddock (1980) approximation and the Parlange et al. (1994) approximation, respectively.

Table 1: Numerical details, associated with the results shown in Fig. 3, for the pseudospectral flux concentration solution (PFCS), the Parlange and Braddock (1980) approximation (Par. 1980) and the Parlange et al. (1994) (Par. 1994) approximation. All three methods employed a Chebyshev differentiation matrix with 100 Chebyshev nodes.

m (-)	ϑ_0 (-)	ϑ_I (-)	σ (-)	% error for σ		Computation time (ms)		
				Par. 1980	Par. 1994	PFCS	Par. 1980	Par. 1994
0.2	0.7	0.001	0.059	0.001	0.002	2.48	0.91	0.97
0.2	0.7	0.3	0.043	0.000	0.048	3.29	0.89	0.88
0.2	0.7	0.6	0.016	0.132	0.140	4.35	0.74	0.92
0.2	1	0.001	0.431	0.013	0.005	2.07	0.85	0.81
0.2	1	0.3	0.359	0.018	0.019	2.33	1.07	1.00
0.2	1	0.6	0.267	0.000	0.118	3.05	3.96	3.02
0.7	0.7	0.001	0.232	0.004	0.019	4.12	1.24	1.26
0.7	0.7	0.3	0.163	0.165	0.175	3.58	1.29	0.91
0.7	0.7	0.6	0.052	0.077	0.082	4.76	1.03	0.95
0.7	1	0.001	1.060	0.038	0.031	2.65	1.07	0.94
0.7	1	0.3	0.882	0.036	0.103	3.03	2.62	2.38
0.7	1	0.6	0.653	0.041	0.281	3.55	1.05	1.33

3.3. Inverse modelling of horizontal infiltration experimental data

Here we show how the pseudospectral flux concentration solution can be used for inverse modelling. Fig. 4 shows plots of observed and simulated moisture content profiles and the cumulative infiltration against time, during horizontal infiltration experiments, for the three soil samples of Villarreal et al. (2019). The solid lines were obtained by calibrating the flux concentration solution, with a van Genuchten diffusivity, to the observed experimental data using the procedure described in Section 2.6. The resulting model parameters are presented in Table 2. Notably, each inversion took around one second to complete using a Lenovo Thinkpad with an Intel Core i5-835OU CPU at 1.70 GHz (exact computation times are also reported in Table 2).

Villarreal et al. (2019) obtained their van Genuchten diffusivity parameters using the finite element code, HYDRUS (Šimunek et al., 2000). For comparison their model parameters are also presented in Table 2.

No specific experimental values of θ_I were given by Villarreal et al. (2019). However, they report that the mean air-dried initial moisture contents were between 0.03 and 0.07 for the three soil types, which is in general agreement with our fitted values for θ_I. In Fig. 4 of Villarreal et al. (2019), it can be seen that their predicted time varying moisture contents, at 15 and 25 cm for all three soils, have a curvature that changes sign as θ approaches θ_s. This type of behaviour is not possible with a numerical solution of Eqs. (1) to (3), nor is it shown in their experimental data. Except for the slight offset in matching the initial moisture contents for the loam and sandy loam soils, our pseudospectral flux concentration solution not only has a far superior match to the experimental data, but it also has the correct mathematical behaviour near θ_s. Villarreal et al. (2019) also had difficulty matching the initial moisture contents but do not comment on this; perhaps the difference is due to the inherent accuracy in the moisture sensors at such a low moisture content.

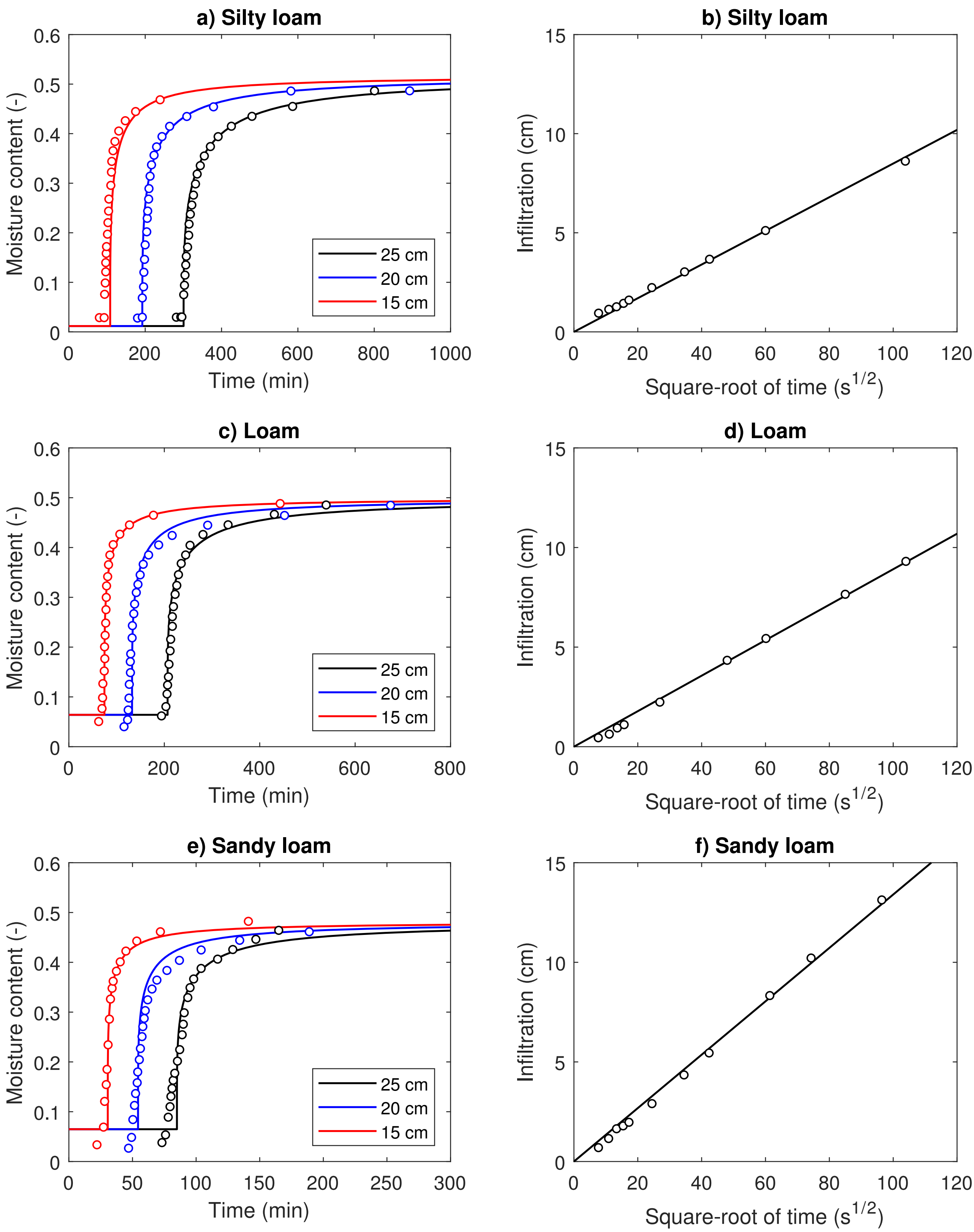

Figure 4: a), c) and e) show plots of moisture content against time at different distances from the inlet boundary of a horizontal infiltration experiment, for the three soils of Villarreal et al. (2019). The circular markers are from the experimental observations made by Villarreal et al. (2019). The solid lines are from the pseudospectral flux concentration solution. b), d) and f) show plots of infiltration volume per unit area of soil sample against the square-root of time for each of the three soil samples. The circular markers are from the experimental observations made by Villarreal et al. (2019). The straight lines are obtained by linear regression.

Table 2: Results from calibrating the pseudospectral flux concentration solution to experimental horizontal infiltration data obtained by Villarreal et al. (2019) along with the model parameters previously estimated by Villarreal et al. (2019).

	Flux concentration solution			Villarreal et al. (2019)		
	Sample 1	Sample 2	Sample 3	Sample 1	Sample 2	Sample 3
S (cm s$^{-1/2}$)	0.0849	0.0891	0.134	0.08	0.08	0.15
m (-)	0.320	0.266	0.236	0.231	0.281	0.438
θ_r (-)	0.0113	0.0636	0.0644	0.05	0.05	0.05
$\theta_s - \theta_r$ (-)	0.508	0.437	0.418	0.46	0.49	0.46
$K_s\psi_c$ (cm^{2}s^{-1})	0.0383	0.0656	0.1890	0.0435	0.0444	0.0505
MAE (min$^{1/2}$cm^2)	0.022	0.021	0.017			
Computation time (s)	0.52	0.55	0.88			

3.4. Application to desorption

Our pseudospectral flux concentration solution can be used to simulate desorption by setting ϑ_0 to be less than ϑ_I. Under such conditions, the cumulative desorption of fluid, V_d [L], through $x = 0$ is found from (Lisle et al., 1987)

$$V_d = \int_0^t D(\theta_0) \left.\frac{\partial \theta}{\partial x}\right|_{x=0} dt = S_d t^{1/2} \tag{54}$$

where S_d [LT$^{-1/2}$] is the desorptivity.

The dimensionless desorptivity, σ_d [-], is found from (Lisle et al., 1987)

$$\sigma_d \equiv \frac{S_d}{\sqrt{(\theta_s - \theta_r) K_s \psi_c}} = \int_{\vartheta_0}^{\vartheta_I} \phi(\vartheta) d\vartheta \tag{55}$$

Note that $\sigma_d^2 = \sigma^2$.

Here we revisit the desorption results previously presented by Lisle et al. (1987) who provided highly accurate numerical solutions for desorptivity using both a power law diffusivity function

$$\overline{D} = (m+1)\vartheta^m \tag{56}$$

and an exponential diffusivity function

$$\overline{D} = \frac{m e^{m\vartheta}}{e^m - 1} \tag{57}$$

where in both cases, m [-] is an empirical exponent.

Dimensionless desorptivity values, σ_d, were calculated using the pseudospectral flux concentration solution when $\vartheta_0 = 0$ and $\vartheta_I = 1$, using both of the diffusivity functions given by Eqs. (56) and (57). In Table 3 we compare our results for both 10 and 100 Chebyshev nodes alongside the numerical results from Lisle et al. (1987).

With just 10 Chebyshev nodes, the pseudospectral flux concentration solution is able to provide higher accuracy, in all but three cases, than the approximate solutions previously studied by Lockington (1994). With 100 Chebyshev nodes, the pseudospectral flux concentration solution provides exact correspondence with the results of Lisle et al. (1987) to four decimal places in all but four cases.

Note that we obtained the numerical results for the exponential diffusivity function, due to Lisle et al. (1987), from Table 2 of Lockington (1994). The original results presented in Table 1 of Lisle et al. (1987) have been scaled in a different way.

Also note that when a power law diffusivity is used with $m = 1$, Table 1 of Lisle et al. (1987) provides a desorptivity value of 0.9382. However, if you take the results from their Table 2 and utilize their Eq. (22), one arrives instead at a desorptivity value of 0.9392, which is the same as the value from our solution with 100 Chebyshev nodes.

Table 3: Dimensionless desorptivity values, σ_d, for different m values, with different diffusivity functions, when $\vartheta_0 = 0$ and $\vartheta_I = 1$. Results were produced using the pseudospectral flux concentration solution with $N = 10$ and $N = 100$. Numerical results due to Lisle et al. (1987) are shown for comparison.

	Power law diffusivity function, Eq. (56)			Exponential diffusivity function, Eq. (57)		
m	$N = 10$	$N = 100$	Lisle et al. (1987)	$N = 10$	$N = 100$	Lisle et al. (1987)
1	0.9391	0.9392	0.9382	1.0424	1.0464	1.0464
2	0.8198	0.8199	0.8199	0.9571	0.9596	0.9595
3	0.7365	0.7366	0.7366	0.8738	0.8753	0.8753
4	0.6743	0.6743	0.6743	0.7980	0.7988	0.7988
5	0.6256	0.6255	0.6255	0.7321	0.7325	0.7325
6	0.5860	0.5860	0.5860	0.6764	0.6765	0.6766
7	0.5532	0.5531	0.5531	0.6296	0.6297	0.6297
8	0.5253	0.5251	0.5251	0.5904	0.5904	0.5903
9	0.5012	0.5010	0.5010	0.5573	0.5572	0.5572
10	0.4802	0.4800	0.4800	0.5290	0.5288	0.5288

4. Summary and conclusions

The objective of this article was to demonstrate the benefits of using a pseudospectral method to solve the horizontal infiltration equation. The non-linear diffusion problem was transformed into a self-similar second-order differential equation, with flux concentration and moisture content as the dependent and independent variables, respectively. The flux concentration formulation was chosen because it provided a scheme whereby both the dependent and independent variables are bounded within finite domains. The resulting boundary value problem was solved within a Newton iteration scheme using a Chebyshev differentiation matrix, leading to a pseudospectral solution of the horizontal infiltration equation. It was also shown how to use a Chebyshev differentiation matrix to evaluate the integrals within the approximate solutions of Parlange and Braddock (1980) and Parlange et al. (1994).

An error analysis was performed by comparison with closed-form exact solutions for two special diffusivity functions, previously provided by Philip (1960). It was demonstrated for the $\phi = 1 - \vartheta^m$ case, that both the Parlange approximations and the pseudospectral flux concentration solution are very accurate. However, for the $\phi = (1 - \vartheta)^m$ case, both of the Parlange approximations retained an irreducible error. In contrast, error associated with the pseudospectral flux concentration solution progressively reduced towards zero with increasing number of Chebyshev nodes. The accuracy of our pseudospectral flux concentration solution is purely dependent on the number of Chebyshev nodes applied.

A comparison between the pseudospectral flux concentration solution and Parlange's approximations was then conducted for a range of parameter values using the van Genuchten (1980) diffusivity function. The approximations provided very accurate moisture content distributions and corresponding estimates for sorptivity with less than 0.3% error.

The pseudospectral flux concentration solution took between two and ten times longer to compute as compared to Parlange's approximations, which was largely due to the Newton iteration scheme that Parlange's approximations do not require. Nevertheless, the pseudospectral method provided an extremely fast means of evaluating both the approximations and the flux concentration solution with computation times for the flux concentration solution being of the order of a few milliseconds. The pseudospectral flux concentration solution was also found to be effective for simulating desorption for both power law and exponential law diffusivities.

Inverse methods are well known for being computationally demanding and faster more accurate and efficient methods are always being sought after. The pseudospectral formulation provides an extremely fast and accurate numerical method that can be used in inverse methods for estimating soil hydraulic parameters. A demonstration was provided whereby van Genuchten (1980) parameters were estimated by model calibration to observed experimental data from horizontal infiltration experiments on three different soil samples, previously presented by Villarreal et al. (2019). Model parameters were iteratively chosen using a simplex algorithm. The model inversion process was found to take around one second using modest laptop computer resources and the resulting model fit to observed data was found to be of very good quality.

References

Babu, D. K. (1976). Infiltration analysis and perturbation methods: 2. Horizontal absorption. Water Resources Research, 12(5), 1013-1018.

Bjørnarå, T. I., & Mathias, S. A. (2013). A pseudospectral approach to the McWhorter and Sunada equation for two-phase flow in porous media with capillary pressure. Computational Geosciences, 17(6), 889-897.

Brutsaert, W. (1976). The concise formulation of diffusive sorption of water in a dry soil. Water Resources Research, 12(6), 1118-1124.

Brooks, R. H., & Corey, A. T. (1964). Hydraulic properties of porous media. Hydrology papers (Colorado State University); no. 3.

Fornberg, B. (1998). A Practical Guide to Pseudospectral Methods (Vol. 1). Cambridge University Press.

Gardner, W. R. (1958). Some steady-state solutions of the unsaturated moisture flow equation with application to evaporation from a water table. Soil Science, 85(4), 228-232.

Hayek, M. (2018). An efficient analytical model for horizontal infiltration in soils. Journal of Hydrology, 564, 1120-1132.

Lagarias, J. C., Reeds, J. A., Wright, M. H., & Wright, P. E. (1998). Convergence properties of the Nelder–Mead simplex method in low dimensions. SIAM Journal on Optimization, 9(1), 112-147.

Lisle, I. G., Parlange, J. Y., & Haverkamp, R. (1987). Exact desorptivities for power law and exponential diffusivities. Soil Science Society of America Journal, 51(4), 867-869.

Lockington, D. A. (1994). Falling rate evaporation and desorption estimates. Water Resources Research, 30(4), 1071-1074.

Ma, D., Wang, Q., & Shao, M. (2009). Analytical method for estimating soil hydraulic parameters from horizontal absorption. Soil Science Society of America Journal, 73(3), 727-736.

McWhorter, D. B., & Sunada, D. K. (1990). Exact integral solutions for two-phase flow. Water Resources Research, 26(3), 399-413.

Parlange, J. Y. (1971). Theory of water-movement in soils: I. One-dimensional absorption. Soil Science, 111(2), 134-137.

Parlange, J. Y. (1973). Horizontal infiltration of water in soils: A theoretical interpretation of recent experiments. Soil Science Society of America Journal, 37(2), 329-330.

Parlange, J. Y. (1975). On solving the flow equation in unsaturated soils by optimization: Horizontal infiltration. Soil

Science Society of America Journal, 39(3), 415-418.

Parlange, J. Y., & Braddock, R. D. (1980). An application of Brutsaert's and optimization techniques to the nonlinear diffusion equation: The influence of tailing. Soil Science, 129(3), 145-149.

Parlange, J. Y., Godaliyadda, G., Fuentes, C., & Haverkamp, R. (1991). Comment on An approximate solution for one-dimensional absorption in unsaturated porous media'by R. W. Zimmerman and G. S. Bodvarsson. Water Resources Research, 27(8), 2159-2160.

Parlange, J. Y., Barry, D. A., Parlange, M. B., Lockington, D. A., & Haverkamp, R. (1994). Sorptivity calculation for arbitrary diffusivity. Transport in Porous Media, 15(3), 197-208.

Parslow, J., Lockington, D., & Parlange, J. Y. (1988). A new perturbation expansion for horizontal infiltration and sorptivity estimates. Transport in Porous Media, 3(2), 133-144.

Piché, R. (2007). Solving BVPs using differentiation matrices. Tampere University of Technology.

Piché, R., & Kanniainen, J. (2009). Matrix-based numerical modelling of financial differential equations. International Journal of Mathematical Modelling and Numerical Optimisation, 1(1-2), 88-100.

Philip, J. R. (1955). Numerical solution of equations of the diffusion type with diffusivity concentration-dependent. Transactions of the Faraday Society, 51, 885-892.

Philip, J. R. (1957). The theory of infiltration: 4. Sorptivity and algebraic infiltration equations. Soil Science, 84(3), 257-264.

Philip, J. R. (1960). General method of exact solution of the concentration-dependent diffusion equation. Australian Journal of Physics, 13, 1.

Philip, J. R. (1969). Theory of infiltration. In Advances in hydroscience (Vol. 5, pp. 215-296). Elsevier.

Philip, J. R. (1973). On solving the unsaturated flow equation: 1. The flux-concentration relation. Soil Science, 116(5), 328-335.

Philip, J. R., & Knight, J. H. (1974). On solving the unsaturated flow equation: 3. New quasi-analytical technique. Soil Science, 117(1), 1-13.

Sadeghi, M., Tabatabaeenejad, A., Tuller, M., Moghaddam, M., & Jones, S. B. (2017). Advancing NASA's AirMOSS P-band radar root zone soil moisture retrieval algorithm via incorporation of Richards' equation. Remote Sensing, 9(1), 17.

Šimunek, J., Hopmans, J. W., Nielsen, D. R., & van Genuchten, M. T. (2000). Horizontal infiltration revisited using parameter estimation. Soil science, 165(9), 708-717.

Su, L., Wang, Q., Qin, X., Shan, Y., & Wang, X. (2017). Analytical solution of a one-dimensional horizontal-absorption equation based on the Brooks–Corey model. Soil Science Society of America Journal, 81(3), 439-449.

Suk, H., & Park, E. (2019). Numerical solution of the Kirchhoff-transformed Richards equation for simulating variably saturated flow in heterogeneous layered porous media. Journal of Hydrology, 579, 124213.

Tzimopoulos, C., Evangelides, C., & Arampatzis, G. (2015). Explicit Approximate Analytical Solution of the Horizontal Diffusion Equation. Soil Science, 180(2), 47-53.

van Genuchten, M. T. (1980). A closed-form equation for predicting the hydraulic conductivity of unsaturated soils. Soil Science Society of America Journal, 44(5), 892-898.

Weideman, J. A., & Reddy, S. C. (2000). A MATLAB differentiation matrix suite. ACM Transactions on Mathematical Software (TOMS), 26(4), 465-519.

Su, L., Wang, Q., Qin, X., Shan, Y., Zhou, B., & Wang, J. (2018). Analytical solution of the one-dimensional nonlinear Richards equation based on special hydraulic functions and the variational principle. European Journal of Soil Science, 69(6), 980-996.

Villarreal, R., Lozano, L. A., Melani, E. M., Salazar, M. P., Otero, M. F., & Soracco, C. G. (2019). Diffusivity and sorptivity determination at different soil water contents from horizontal infiltration. Geoderma, 338, 88-96.

Zimmerman, R. W., & Bodvarsson, G. S. (1989). An approximate solution for one-dimensional absorption in unsaturated porous media. Water Resources Research, 25(6), 1422-1428.

Appendix A. MATLAB implementation of the pseudospectral flux concentration solution

Below is a short MATLAB script that can be used to determine both σ and ϕ for a given scenario using the psuedospectral flux concentration solution.

```
N=100; %Number of Chebyshev nodes
thI=0.001; %Initial moisture content
th0=0.7; %Boundary moisture content
m=0.2; %van Genuchten parameter
[z,D]=chebdif(N,2); %Get differentitation matrices
dzdth=2/(th0-thI); %Chebyshev node scaling factor
E1=dzdth*D(:,:,1); %First-order
E2=dzdth^2*D(:,:,2); %Second-order
%Determine coefficients for integration
IntCoefs=pi/(N-1)/dzdth*sqrt(1-z.^2)';
I=eye(N); %Identity matrix
%Determine theta values for each z value
th=(th0+thI)/2+(th0-thI)/2*z;
%Determine diffusivity for each z value
L=(1-th.^(1/m)).^m;
Dbar=(1-m)/m*th.^(0.5-1/m).*(1-L).^2./L;
OF=1; %Initialise objective function
i=2:N-1; %Inner node index
F=ones(N,1); %Initial guess
while OF>1e-6 %Newton iteration
%Determine square of sorptivity
sig2=IntCoefs*[2*(th-thI).*Dbar./F];
Q=2*Dbar/sig2./F;
R=[E2(i,:)*F+I(i,:)*Q;F(N)-0;F(1)-1];
dR=[E2(i,:)+I(i,:)*diag(-Q./F);I(N,:);I(1,:)];
Fold=F; %Store previous iteration
F=max(eps,F-dR\R); %Update F and ensure > 0
OF=max(abs(F-Fold)); %Define objective function
end
%Determine phi for each theta value
phi=sqrt(sig2)*E1*F;
```